Engineering 31 (2023) 59–69

Contents lists available at ScienceDirect

Engineering

journal homepage: www.elsevier.com/locate/eng

Research
Environmental Engineering—Article

The Successional Pattern of Microbial Communities and Critical Genes of Consortia Subsisting on Chloramphenicol and Its Metabolites Through Long-Term Domestication

Jiayu Zhang [a,b,c,d], Kaiyan Zhou [a,b,c], Fangliang Guo [a,b,c], Huaxin Lei [a,b,c], Renxin Zhao [a,b,c], Lin Lin [a,b], Xiaoyan Li [a,b], Bing Li [a,b,*]

[a] State Environmental Protection Key Laboratory of Microorganism Application and Risk Control, Tsinghua Shenzhen International Graduate School, Tsinghua University, Shenzhen 518055, China
[b] Shenzhen Engineering Research Laboratory for Sludge and Food Waste Treatment and Resource Recovery, Tsinghua Shenzhen International Graduate School, Tsinghua University, Shenzhen 518055, China
[c] School of Environment, Tsinghua University, Beijing 100084, China
[d] Research Center for Eco-Environmental Engineering, Dongguan University of Technology, Dongguan 523808, China

ARTICLE INFO

Article history:
Received 13 January 2023
Revised 19 May 2023
Accepted 11 July 2023
Available online 25 August 2023

Keywords:
Antibiotic
Biodegradation
Metabolism
Microbial community succession
Metagenome

ABSTRACT

As a widespread emerging contaminant, chloramphenicol (CAP) adversely impacts ecological communities in the water environment. Biological treatment is widely used for aquatic pollutant removal, and the performance of functional microbes determines its outcome. Herein, a consortium with a powerful CAP-degrading capacity was domesticated from activated sludge. As the common degradation products of CAP, 4-nitrobenzoic acid (PNB) and 2,2-dichloroacetic acid (DCA) were also used as the sole substrates for long-term domestication. The successional pattern of the microbial community and critical functional genes through the 2.5-year domestication was revealed by metagenomic analysis. *Sphingomonas*, *Caballeronia*, and *Cupriavidus* became the most dominant populations in the CAP-, PNB-, and DCA-degrading consortia, respectively, and they were crucial degraders of PNB and DCA. Their collaboration contributed to the high mineralization rate of CAP. PNB was transformed into protocatechuic acid (PCA) and then mineralized through meta-cleavage and ortho-cleavage pathways. Crucial functional genes involved in CAP, PNB, and DCA metabolism, including CAP acetyltransferase, CAP oxidoreductase, haloacid dehalogenases, and protocatechuate dioxygenases, were significantly enriched in consortia. pH and carbon source had significant impacts on CAP biodegradation efficiency. The domesticated consortia and isolated strains are necessary microbial resources to enhance the bioremediation of CAP-, PNB-, or DCA-polluted environments.

1. Introduction

Antibiotics play a crucial role in antibacterial treatment in clinics. However, along with excessive consumption, their residues are continuously entering into the environment. Significantly, wastewater from pharmaceutical factories, hospitals, and livestock and aquaculture farms is a main source of antibiotic contamination [1–3]. The persistence of antibiotics in aquatic environments negatively impacts ecological communities and facilitates the development and spread of antibiotic resistance genes, which challenges clinical anti-infective therapy [4–6]. Removing antibiotics from wastewater can effectively reduce their transfer into the environment, which has become an arduous task in the environmental engineering field [7]. Biological treatment systems are commonly applied to remove organic pollutants in wastewater treatment plants (WWTPs). Microbes play a crucial role in removing organic contaminants in engineered environments, and their performance determines the outcomes of biological treatment systems [8]. The emergence and prevalence of vigorous antibiotic-degrading microbes will dramatically enhance the removal efficiency of antibiotics in biological treatment systems. The activated sludge microbiome, which is regularly exposed to elevated antibiotic concentrations in wastewater, might serve as a promising resource of

* Corresponding author.
E-mail address: bingli@sz.tsinghua.edu.cn (B. Li).

https://doi.org/10.1016/j.eng.2023.07.009

antibiotic-degrading microbes that could subsequently be applied in the environmental remediation biotechnology of chloramphenicol (CAP)-contaminated environments. Activated sludge domestication through feeding with the corresponding antibiotic is a conventional approach to remodeling the microbiota with a puissant antibiotic-degrading capacity [9]. Researchers have commonly focused on domesticated communities' functions and microbial structure rather than community succession during domestication [10,11]. Determining the processes of microbial community domestication will aid in expanding our knowledge of the successional patterns of microbial communities feeding on antibiotics and provide important information for improving the strategy for microbial community domestication.

As a broad-spectrum antibiotic, CAP is heavily consumed in clinical practice and livestock and aquiculture production in some developing countries owing to its effectiveness and low cost [2]. CAP is refractory in wastewater biotreatment systems of WWTPs because of its bacteriostatic activity by inhibiting protein synthesis [12]. Herein, we characterized a vigorous CAP-degrading consortium with the potential for application in the enhancement of CAP biotreatment. In our previous study, a comprehensive CAP metabolic pathway was clarified, and 4-nitrobenzoic acid (PNB) and 2,2-dichloroacetic acid (DCA) were proven to be the main CAP biodegradation products produced by this consortium [13]. In addition, several studies also pointed out that PNB and DCA were the most common products of CAP in both biological and chemical treatment processes [12,14–16]. The residues of PNB and DCA can induce genotoxicity and developmental toxicity in organisms [17]. In particular, DCA is also a common noxious disinfection byproduct that generated in the disinfection processes such as chlorination [18]. It has already been included in drinking water regulations and guidelines in many countries such as China, the United States, and Canada, because of its adverse effects on human health [19]. Thus, it is valuable to domesticate consortia or isolate powerful microbial degraders for efficient DCA and PNB removal from the water environment. The current study was conducted to ① investigate the successional pattern of the CAP-degrading microbial consortium derived from activated sludge during 2.5 years of domestication through metagenomic analysis; ② characterize the CAP, PNB, and DCA degrading capacities of the domesticated consortia and isolated strains; ③ decipher the dynamic changes in essential functional enzyme-encoding genes involved in CAP, DCA, and PNB biotransformation; and ④ reveal the impacts of environmental and nutrient factors on CAP biodegradation and the microbial community.

2. Materials and methods

2.1. The procedures of consortium domestication

Previously, activated sludge bioreactors treating CAP production wastewater and control bioreactors treating wastewater without CAP were initially established to investigate the development of antibiotic resistance genes in activated sludge under antibiotic selection pressure [20]. Herein, they were included in the investigation of the successional pattern of a microbial community subsisting on CAP. A panorama of the entire time course of CAP-subsisting consortium domestication was demonstrated for the first time. The seed activated sludge of these bioreactors was collected from a local municipal WWTP. Detailed information about the operation of these bioreactors has been described in a previous study [20]. CAP concentrations in wastewater increased stepwise from 20 to 120 $mg{\cdot}L^{-1}$ according to their removal behaviors during successive domestication. After approximately 5.5 months, the consortium could steadily degrade 120 $mg{\cdot}L^{-1}$ CAP in wastewater and was then inoculated into synthetic mineral salt medium (MSM) containing 120 $mg{\cdot}L^{-1}$ CAP for further domestication to simplify the community. The compositions of MSM were reported in our previous study [13]. After approximately 12 months, the consortium was inoculated into MSM containing 100 $mg{\cdot}L^{-1}$ PNB or DCA for another 12-month domestication to enrich microbes with the ability to utilize PNB and DCA. CAP, PNB, and DCA were supplied as the sole carbon source, and 30 $mg{\cdot}L^{-1}$ NH_4Cl was supplied as a nitrogen source for consortium domestication in MSM. Finally, three consortia named CL-CAP, CL-PNB, and CL-DCA with the ability to utilize CAP, PNB, and DCA as the sole carbon source were successfully domesticated. All cultivation was conducted at 25 °C and 120 revolutions per minute ($r{\cdot}min^{-1}$) shaking in batch mode. The culture medium was renewed every 3–5 d according to the consumption of substrates. In this study, 16 microbial samples at each domestication stage were collected for DNA extraction and metagenomic sequencing across the domestication process. In addition, 46 metagenomic datasets of consortium CL-CAP reported in our previous studies [20–22] were included for metagenomic analysis with totally different research objectives in this study. Information about all of the involved samples and metagenomic datasets is listed in Table S1 in Appendix A.

2.2. Batch biodegradation experiments

Batch biodegradation experiments of CAP, PNB, and DCA by the domesticated CAP-, PNB-, and DCA-degrading consortia were conducted. Cells of the consortia were collected during the batch experiments for metagenomic sequencing. Eight strains were isolated from the domesticated consortium using mineral salt and R2A agar plates amended with CAP [13,21], and they were included for the analysis of their contribution to PNB and DCA biodegradation in the consortium.

To investigate the impacts of various nutrient conditions on the CAP biodegradation performance of the domesticated consortium, MSMs amended with various additional carbon sources (including sodium acetate, sodium citrate, sodium pyruvate, and sodium benzoate at concentrations of 2.4, 12, and 60 $mmol{\cdot}L^{-1}$), additional nitrogen sources (including NH_4Cl, $NaNO_2$, and $NaNO_3$ at 0.56 $mmol{\cdot}L^{-1}$), and initial CAP concentration ranging from 50 to 600 $mg{\cdot}L^{-1}$ were used for batch experiments of CAP biodegradation. Moreover, the impacts of inoculum size (5%, 15%, and 25% of the culture medium volume), pH (3.5, 4.5, 6.0, 7.5, and 8.5), and temperature (20, 25, and 30 °C) on CAP biodegradation by the domesticated consortium were also investigated. Culture cells were collected for 16S ribosomal ribonucleic acid (rRNA) amplicon sequencing at 36 and 72 h after inoculation, except for cultures in MSM amended with sodium benzoate or at pH 3.5 and 8.5 because of their slow growth. Detailed information about these collected samples is listed in Table S2 in Appendix A.

All batch experiments were conducted in triplicate as follows. The cells of domesticated consortium or isolated pure cultures were collected via centrifugation and washed with fresh MSM three times. Then, the collected cells were inoculated into MSM containing the corresponding substrates for batch biodegradation experiments. Liquid samples were collected at intervals for chemical analysis. They were filtered with 0.22 μm polytetrafluoroethylene (PTFE) syringe filters (ANPEL Laboratory Technologies Inc., China). The optical density at 600 nm (OD_{600}) of cultures was determined by an Infinite M200 microplate reader (Tecan, Switzerland).

2.3. Chemical analysis

The soluble total organic carbon (TOC) was determined via a TOC-L analyzer (Shimadzu Corporation, Japan). When CAP, PNB,

or DCA was supplied as the sole carbon source in the culture medium, the TOC reduction rate could represent their mineralization rate. The final mineralization rate was calculated as the percentage of TOC reduction. CAP, PNB, protocatechuic acid (PCA), and DCA were detected and quantified by a high-performance liquid chromatography (HPLC)-quadrupole time-of-flight (QTOF)-mass spectrometer (MS) (Impact II™; Bruker, Germany) equipped with a Thermo Hypersil Gold column (100 mm × 2.1 mm, 1.9 μm) (Thermo Fisher Scientific, USA) according to our previously established method [13]. Eluent A of HPLC was Milli-Q water containing 5 mmol·L^{-1} ammonium acetate, and eluent B was methanol. The gradient elution process in HPLC is shown in Table S3 in Appendix A. The MS was operated in negative ionization mode, and the detailed operating parameters for chemical identification and quantification were described in a previous study [13]. A reference solution was injected for mass-to-charge ratio (m/z) calibration. Chemicals were analyzed in scan mode, and the chemical structure was further confirmed according to their fragmentation patterns determined in product ion scan mode.

2.4. DNA extraction, metagenomic, and 16S rRNA amplicon sequencing

Both short-read metagenomes through Illumina sequencing and long-read metagenomes through Oxford nanopore technologies (ONT) sequencing were acquired in this study. The total DNA of microbial samples for Illumina metagenomic sequencing and 16S rRNA amplicon sequencing was extracted using the FastDNA™ Spin Kit for Soil (MP Biomedicals, USA) following the manufacturer's manual. The total DNA of microbial samples for ONT sequencing was extracted using the DNeasy PowerSoil Kit (Qiagen, USA) following the manufacturer's recommendations. The extracted DNA was checked by 1% agarose gel electrophoresis and a Qubit® 2.0 Fluorometer (Life Technologies, USA). Illumina metagenomic sequencing libraries were constructed using the NEBNext® Ultra™ DNA Library Prep Kit for Illumina (NEB, USA) following the manufacturer's instructions. The libraries were sequenced on the Illumina NovaSeq platform using a paired-end (PE) 150 base pairs (bp) strategy at Novogene (China). The construction of the ONT metagenomic sequencing library was performed using the Ligation Sequencing 1D kit (SQK-LSK109) (ONT, UK) following the manufacturer's recommendations. The ONT library was sequenced on a PromethION (ONT) platform at Novogene (China). Information on 62 short-read metagenomic datasets and ten long-read metagenomic datasets is listed in Table S1. Metagenomic datasets were deposited to PRJNA953649 of the National Center for Biotechnology Information (NCBI) Sequence Read Archive (SRA) database.

16S rRNA amplicon sequencing of 104 samples was performed to characterize the microbial community of the consortium under various culture conditions. The V4 region was amplified using primers 515F (5′-GTGCCAGCMGCCGCGG-3′) and 806R (5′-GGACTACHVGGGTWTCTAAT-3′) on an ABI GeneAmp® 9700 polymerase chain reaction (PCR) instrument (Applied Biosystems, USA). The TransStart® FastPfu DNA Polymerase AP221-01 Kit (TransGen Biotech, China) was used for PCR. A 20 μL PCR system consisted of 10 ng of template DNA, 0.8 μL of each primer at 5.0 μmol·L^{-1}, 2.0 μL of 2.5 mmol·L^{-1} deoxy-ribonucleoside triphosphates (dNTPs), 4 μL of FastPfu buffer, and 0.4 μL of FastPfu polymerase. The PCR procedures were as follows: initial denaturation at 95 °C for 3 min, 27 cycles of denaturation at 95 °C for 30 s, annealing at 55 °C for 30 s, elongation at 72 °C for 45 s, and a final extension at 72 °C for 10 min. The amplified products were purified using 2% agarose gel and an AxyPrep DNA Gel Extraction Kit (Axygen Biosciences, USA). The purified products were quantified using QuantiFluor™ ST (Promega, USA). Then, they were sequenced on the Illumina MiSeq platform with a PE 300 bp strategy at Majorbio (China), and the sequencing depth was an average of approximately 50 000 sequences per sample. 16S rRNA amplicon datasets were deposited to PRJNA953665 of the NCBI SRA database.

2.5. Metagenomic data analysis

Clean Illumina reads were acquired through quality control using fastp (v0.23.2) [23]. The taxonomy of metagenomic data was classified via Kraken2 (v2.1.2) [24], and the abundance of each taxonomic level was estimated via Bracken (v2.7) [25]. Shannon and Pielou's evenness indices of the microbial community were calculated using R (v4.1.2). Principal coordinate analysis (PCoA) of samples was performed based on Bray–Curtis distances of communities.

The Illumina reads were assembled using metaSpades (v3.15.4) [26]. The ONT long reads were filtered through Filtlong with a minimum length threshold of 500 bp and a minimum mean quality weight threshold of ten. The filtered ONT long reads were assembled using metaFlye (v2.9) [27]. The long-read assemblies were polished using Medaka (v1.6.1), Rcon (v1.4.3), and Pilon (v1.24) [28] to obtain high-quality ONT long-read assemblies. Both the short-read and long-read assembled contigs of the final domesticated consortia CL-CAP, CL-PNB, and CL-DCA were assigned to metagenomic assembled genomes (MAGs) via a binning approach using BASALT [29]. MAGs were dereplicated by dRep (v2.0.0) [30] with the following parameters: -sa 0.95 -nc 0.30 -comp 50 -con 10. The completeness and contamination of MAGs were estimated using CheckM (v1.2.0) [31]. The taxonomic classification of MAGs was performed using GTDB-Tk (v2.1.0) [32]. The genes in MAGs were predicted by Prodigal (v2.6.3) [33] and annotated by Prokka (v1.14.5) [34] and KofamKOALA [35]. Replication rates of MAGs were estimated by CoPTR (v1.1.2) [36]. The relative abundances of MAGs in metagenomes were calculated using CoverM (v0.6.1) with the following parameters: genome -m relative_abundance –min-read-aligned-percent 0.75 –min-read-percent-identity 0.95. The significance of the enrichment of each MAG in consortia was determined by the R package limma [37]. The relative abundances of selected genes were calculated as follows: First, the aligned read number per base of selected genes was calculated by CoverM with select genes as reference using the following parameters: contig –m reads_per_base –min-read-aligned-percent 0.75 –min-read-percent-identity 0.95. Then, the output was normalized by dividing by the total read number of a dataset to obtain the relative abundance (coverage, ×/Gb) of the selected genes [20].

2.6. 16S rRNA amplicon sequencing data analysis

The 16S rRNA amplicon sequencing data were analyzed by the QIIME2 platform [38]. The sequences were split and filtered, and then the deblur method was used to denoise and cluster the sequences to generate the operational taxonomic unit (OTU) table. The taxonomy of each representative sequence was annotated by the Ribosomal Database Project (RDP; v2.11) [39] with a confidence threshold of 80%. Redundancy analysis (RDA) and adonis tests were conducted to determine the impacts of environmental and nutrient factors, including the pH, temperature, inoculum size, initial CAP concentration, and initial additional carbon and nitrogen sources, on the microbial community structures using R (v4.1.2).

3. Results and discussion

3.1. Three domesticated consortia with robust CAP, PNB, and DCA degrading ability

The degrading ability of three domesticated consortia for CAP, PNB, and DCA was depicted in Fig. 1. Through 2.5 years of domestication with CAP, the final domesticated consortium CL-CAP could completely degrade 250 mg·L^{-1} CAP with a mineralization rate of 93.7% in 36 h (Figs. 1(a) and (d)). A comprehensive metabolic pathway of CAP was elucidated in our previous study, and PNB and DCA were found to be the main downstream products of CAP produced by this consortium [13]. It has been reported that PNB and DCA are the most common products of CAP in biological treatment processes [12,13,16]. In addition, they were also widely detected in the chemical treatment processes of CAP, such as electrochemical degradation and advanced oxidation processes [14,15,40,41].

As a kind of nitrobenzene compound, PNB is an important raw material and mid-product for industrial manufacture. However, its residues in industrial effluents should be eliminated before discharge into the environment because of its genotoxicity and refractory properties [17,42]. DCA, a haloacetic acid (HAA), is a common noxious disinfection byproduct with cytotoxic, carcinogenic, genotoxic, teratogenic, and mutagenic properties [18,43]. The formation and elimination of HAAs have aroused broad public concern and have been extensively investigated recently [44,45]. Herein, two consortia named CL-PNB and CL-DCA were domesticated from CAP-degrading consortia by feeding on PNB and DCA for 12 months, respectively. Consortium CL-PNB completely degraded 250 mg·L^{-1} PNB with a mineralization rate of 95.9% in 14 h (Figs. 1(b) and (e)). Consortium CL-DCA completely degraded 100 mg·L^{-1} DCA with a mineralization rate of 91.0% in 8 h (Figs. 1(c) and (f)). They demonstrated efficient degradation capacity and have the potential to enhance the bioremediation of PNB- and DCA-polluted environments.

3.2. The recovered MAGs and isolated strains of the domesticated consortia

By virtue of the binning approach on both short-read and long-read metagenomes, 21 MAGs were recovered from three domesticated consortia (i.e., CL-CAP, CL-PNB, and CL-DCA) (Fig. 2(a)). Three of them (MAG4, MAG5, and MAG6) were complete and consisted of only one circular contig (Figs. 2(b) and (c)). Thirteen MAGs were of high quality with completeness higher than 95.0% and contamination less than 3.5% (Fig. 2(c)). MAG1, MAG2, MAG3, MAG4, and MAG5 assigned to genera *Sphingomonas*, *Cupriavidus*, *Caballeronia*, *Pigmentiphaga*, and *62-47* were dominant (average relative abundance > 1.0%) in consortium CL-CAP (Fig. 2(a)). MAG2 (*Cupriavidus*), MAG3 (*Caballeronia*), and MAG4 (*Pigmentiphaga*) were dominant in consortium CL-PNB, while MAG2 (*Cupriavidus*) and MAG5 (*62-47*) were dominant in consortium CL-DCA (Fig. 2(a)). MAG1 (*Sphingomonas*), MAG2 (*Cupriavidus*), and MAG3 (*Caballeronia*) were significantly ($p < 0.05$) enriched in consortia CL-CAP, CL-DCA, and CL-PNB with average relative abundances of 58.6%, 92.5%, and 76.5% in the corresponding consortium, implying that they were crucial bacteria responsible for CAP, DCA, and PNB biodegradation, respectively (Fig. 2(a) and Fig. 3). Replication rates of microbial populations, including MAG1, MAG2, and MAG3, manifested as a reversed-U shaped pattern (Fig. 2(a)). This result suggested that MAG1, MAG2, and MAG3 grew and reproduced actively during CAP, DCA, and PNB reduction, which also implied their crucial roles in the biodegradation of these three compounds.

Our previous study confirmed that *Sphingomonas* sp. CL5.1 isolated from consortium CL-CAP was a crucial CAP degrader that could catabolize CAP to PNB and DCA [13]. Herein, the PNB- and CAP-degrading capacity of eight strains isolated from consortium CL-CAP was investigated, and the results were shown in Fig. 3. *Sphingomonas* sp. CL5.1, *Caballeronia* sp. CLC5, and *Caballeronia* sp. PC1 were PNB degraders who could utilize PNB as the sole carbon source (Fig. 3(a)). *Cupriavidus* sp. CLC6 could also degrade PNB

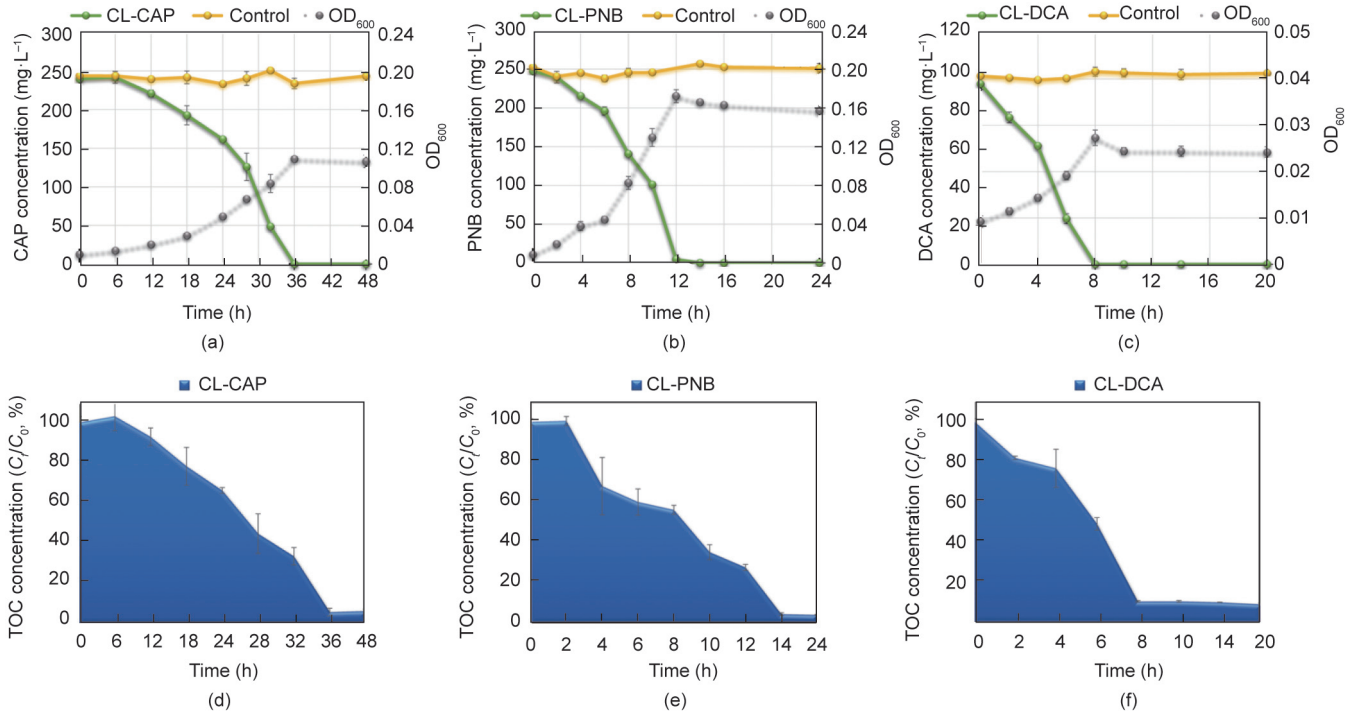

Fig. 1. The performance of three consortia on CAP, PNB, and DCA biodegradation after domestication. (a–c) CAP, PNB, and DCA degradation by enriched consortia CL-CAP, CL-PNB, and CL-DCA, respectively. (d–f) CAP, PNB, and DCA mineralization by enriched consortia CL-CAP, CL-PNB, and CL-DCA, respectively. The initial concentrations of CAP, PNB, and DCA were 250, 250, and 100 mg·L^{-1}, respectively. Values are presented as means ± standard deviation (SD) of three replicates. C_t: concentration value at time t; C_0: initial concentration value at 0 h.

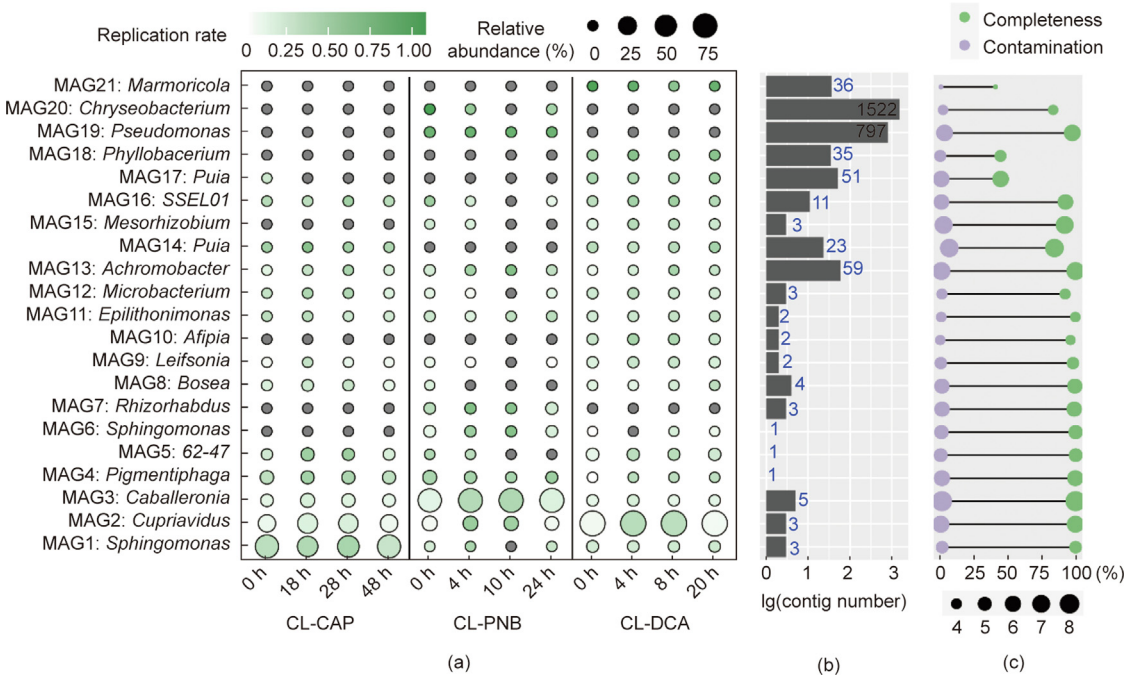

Fig. 2. The features and relative abundances of MAGs in CAP, PNB, and DCA degrading consortia after domestication. (a) The variations of relative abundances and replication rates of MAGs in CAP, PNB, and DCA degrading consortia during the biodegradation process; (b) contig number of each MAG; (c) completeness, contamination, and genome size of each MAG.

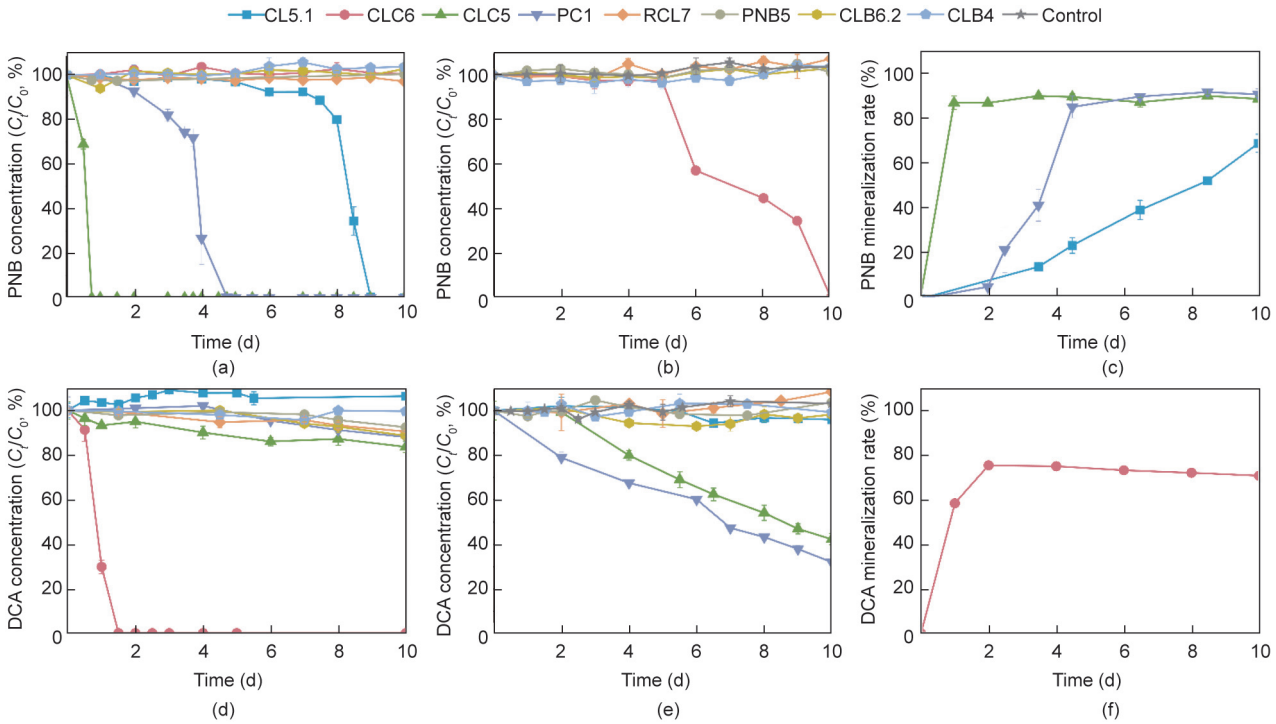

Fig. 3. The biodegradation of PNB and DCA by eight isolated strains including *Sphingomonas* sp. CL5.1, *Cupriavidus* sp. CLC6, *Caballeronia* CLC5, *Caballeronia* sp. PC1, *Chryseobacterium* sp. RCL7, *Labrys* sp. PNB5, *Pigmentiphaga* sp. CLB6.2, and *Achromobacter* sp. CLB4. (a, d) The biodegradation of PNB and DCA as the sole corban source by eight isolated strains. (b, e) The biodegradation of PNB and DCA in the presence of 500 mg·L^{-1} sodium pyruvate. (c, f) The mineralization of PNB and DCA by strains that could utilize them as the sole carbon source. The initial concentrations of PNB and DCA were both 100 mg·L^{-1}. Values are presented as means ± SD of three replicates.

through cometabolism with sodium pyruvate (Fig. 3(b)). Among them, *Caballeronia* sp. CLC5 was the most vigorous PNB degrader, as it could completely degrade 100 mg·L^{-1} PNB in 18 h with a mineralization rate of 89.7% (Figs. 3(a) and (c)). *Cupriavidus* sp. CLC6 was a powerful DCA degrader that could completely degrade 100 mg·L^{-1} DCA in 36 h with a mineralization rate of 70.7% (Figs. 3(d) and (f)), while *Caballeronia* sp. CLC5 and *Caballeronia* sp. PC1 could also degrade DCA through cometabolism with

sodium pyruvate (Fig. 3(e)). Thus, we concluded that *Caballeronia* sp. and *Cupriavidus* sp. were the main contributors to the catabolism of PNB and DCA converted from CAP by *Sphingomonas* sp. in consortium CL-CAP. In other words, they collaborated to mineralize CAP in the consortium. These results of pure culture biodegradation tests confirmed the conjecture on the substrate utilizing preferences of predominant members in communities via metagenomic analysis (Fig. 2(a) and Fig. S1 in Appendix A).

3.3. The successional pattern of microbial communities subsisting on CAP and its metabolites

The microbial composition across the whole domestication process was revealed by the taxonomy classification of short reads. As shown in Fig. 4, 70.22% of the short reads of all samples were successfully classified as bacteria (70.12%), archaea (0.04%), eukaryota (0.05%), and viruses (0.01%). The communities mainly consisted of *Proteobacteria* (63.57%), *Actinobacteria* (4.54%), and *Bacteroidetes* (0.87%) at the phylum level (Fig. 4). The microbial diversity and evenness of consortia decreased through domestication, as the alpha diversity indices (Shannon and Pielou's evenness indices) of the consortia significantly decreased after domestication compared with that of the original seed activated sludge (*t* test, $p < 0.05$) (Figs. 5(a) and (b)). In addition, the community structure was more simplified after domestication in MSM with CAP, PNB, or DCA, as the alpha diversity indices significantly decreased after domestication for more than six months in MSM (*t* test, $p < 0.05$). Similarly, Luan et al. [46] found that the alpha diversity of the aerobic biofilm reactor markedly decreased because of long-term treatment with streptomycin for 576 d. The PCoA ordination of the communities at the genus level across the domestication process revealed that the microbial community was significantly impacted by the culture medium composition (Adonis test, $p < 0.001$) (Fig. S2(a) in Appendix A). For instance, the microbial community markedly changed after being fed with PNB or DCA (Pairwise Adonis test, $p < 0.01$) (Fig. S2(b) in Appendix A). After laboratory domestication with municipal wastewater for 5.5 months, the control consortium (Control-7) without CAP exposure was mainly composed of *Alicycliphilus* (19.9%), *Acidovorax* (10.1%), *Diaphorobacter* (6.3%), *Comamonas* (4.5%), and *Pseudomonas* (3.1%) at the genus level (Fig. 5(c)). At the incipient stage of domestication with 20 $mg \cdot L^{-1}$ CAP, *Paenarthrobacter* (46.0%), *Alicycliphilus* (4.4%), and *Microbacterium* (4.2%) prevailed in the community (CAP-20) (Fig. 5(d)). After domestication with stepwise increasing CAP concentrations for 5.5 months, *Paenarthrobacter* (13.9%), *Sphingomonas* (12.9%), and *Caballeronia* (6.8%) became predominant in the community (CAP-120) (Fig. 5(d)). Finally, through another two-year domestication in the MSM, *Sphingomonas* (57.8% in CAP-120c), *Caballeronia* (60.2% in PNB-100), and *Cupriavidus* (74.5% in DCA-100) became dominators in the communities subsisting on CAP, PNB, and DCA, respectively (Fig. 5(d)). *Sphingomonas*, *Caballeronia*, and *Cupriavidus* were the key degraders of CAP, PNB, and DCA, respectively, which was proven by biodegradation tests using the corresponding pure cultures in this study and our previous study [13]. They became prevalent by virtue of their advantage of substrate utilization in communities feeding on CAP, PNB, and DCA, respectively.

3.4. Dynamic changes in critical genes involved in CAP, DCA, and PNB biotransformation

Our previous study found that CAP was mainly degraded via acetylation and oxidization by the consortium CL-CAP [13]. Acetylation is a common CAP-resistant pathway for bacteria because the

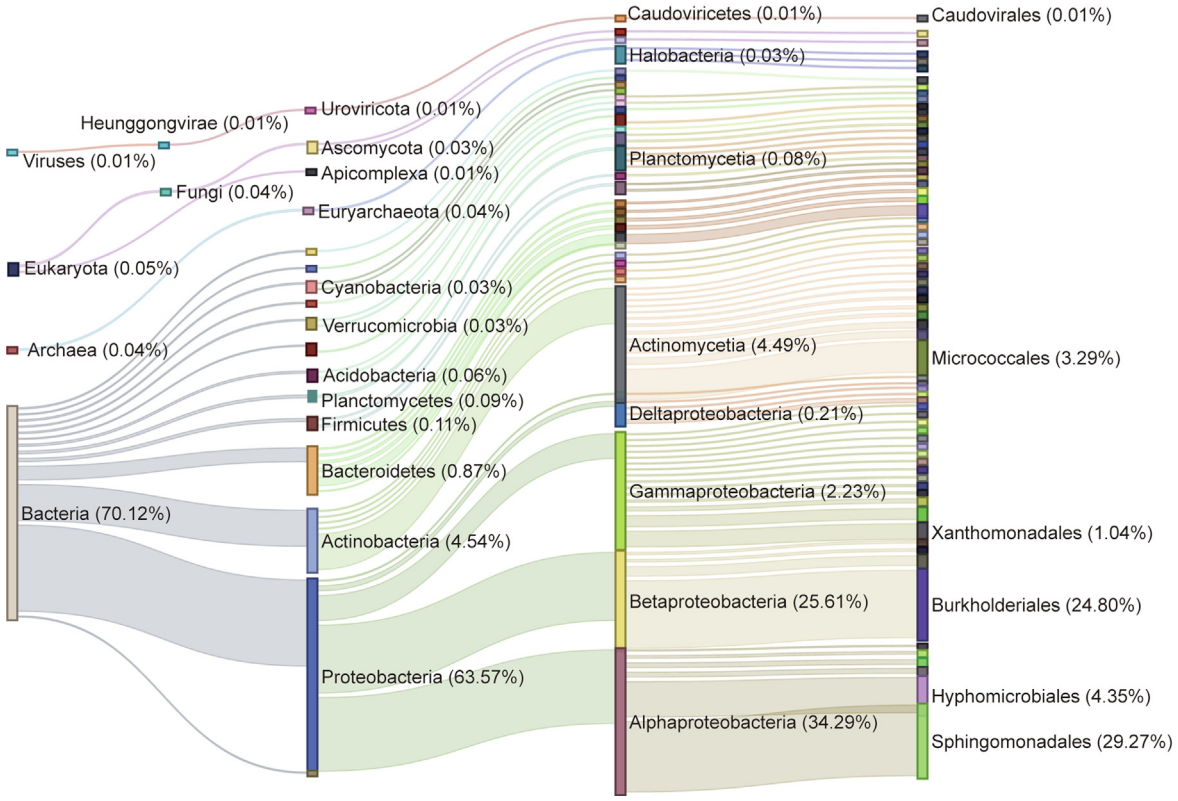

Fig. 4. The taxonomical structure from kingdom to order levels of the microbial communities throughout the whole domestication stage. The thickness of a link indicates the average relative abundance of a taxonomy.

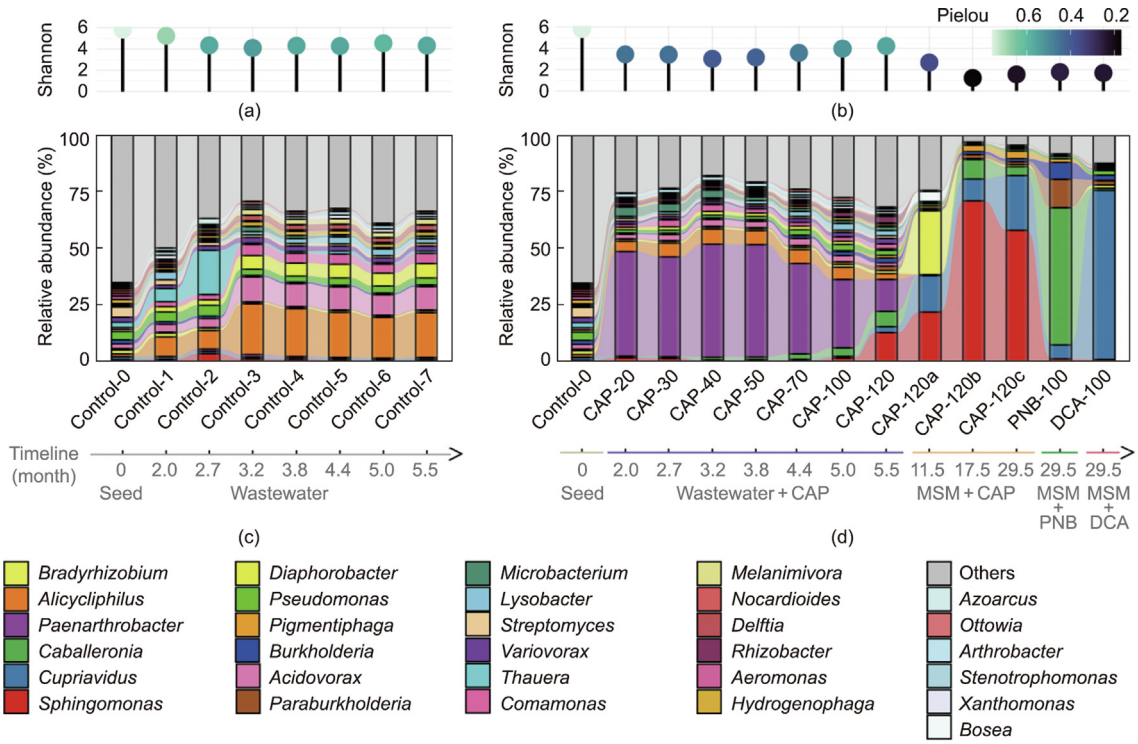

Fig. 5. The microbial succession of the communities during the 2.5-year domestication. (a) Shannon and Pielou's evenness indices of the control consortium communities; (b) Shannon and Pielou's evenness indices of the consortium communities enriched by CAP, PNB, and DCA, respectively; (c) average relative abundances of dominant genera in the control consortium communities; (d) average relative abundances of dominant genera in the consortium communities enriched by CAP, PNB, and DCA, respectively. Values are presented as means of samples in each group.

biodegradation product CAP 3-acetate loses antibacterial activity [47]. The gene *catB3* encoding CAP acetyltransferase, which is responsible for CAP acetylation, was discovered in MAG2 (*Cupriavidus*). The average relative abundance of *catB3* was 3.7 in the control consortium without CAP exposure as shown in Fig. 6. When domesticated with wastewater and then synthetic MSM containing CAP, the average relative abundance of *catB3* increased from 4.0 to 62.4. The oxidization of the hydroxyl group to the carboxyl group at C_3 of CAP was a CAP biodegradation pathway reported recently by our team [13,48] and Ma et al. [12]. The oxidoreductase capO belonging to the glucose–methanol–choline (GMC) oxidoreductase superfamily was discovered to catalyze the two-step oxidation of CAP into oxidized CAP in *Sphingomonas* sp. CL5.1 in previous studies [48,49]. The relative abundance of *capO* was less than 0.05 in the control consortium without CAP exposure. When domesticated with wastewater and then synthetic MSM containing CAP, the average relative abundance of *capO* increased from 25.4 to 341.6.

Haloacid dehalogenases, which can catalyze the hydrolysis of the carbon–chlorine bond in DCA, widely exist in aerobic bacteria [50,51]. This study discovered 15 gene sequences belonging to four types of haloacid dehalogenase-encoding genes (including *dhlB*, *dehI*, *dehII*, and *hdl IVa*) in community members, including MAG2 (*Cupriavidus*), MAG3 (*Caballeronia*), MAG5 (*62-47*), MAG8 (*Bosea*), MAG10 (*Afipia*), MAG13 (*Achromobacter*), and MAG15 (*Mesorhizobium*). There were four haloacid dehalogenase-encoding genes in the genome of MAG2 (*Cupriavidus*), and they were at higher relative abundances in consortium CL-DCA than in other consortia (*t* test, $p < 0.05$). In fact, the isolated strain *Cupriavidus* sp. CLC6 indeed exhibited a strong DCA-degrading ability.

PCA was detected to be a product of PNB produced by consortium CL-PNB, and its structure was further confirmed by PCA standards using HPLC-QTOF-MS (Figs. S3(a) and (b) in Appendix A). PCA was produced during PNB biodegradation and finally mineralized by consortium CL-PNB (Fig. S3(c) in Appendix A). Herein, the PCA-degrading capacity of isolated PNB degraders was also tested. The isolated PNB degraders, including *Sphingomonas* sp. CL5.1, *Caballeronia* sp. PC1, and *Caballeronia* sp. CLC5 could utilize PCA as the sole carbon source (Fig. S3(d) in Appendix A). In particular, *Caballeronia* sp. PC1 and *Caballeronia* sp. CLC5 completely degraded 10 $mg \cdot L^{-1}$ PCA in 8 h. These results suggested that PNB was transformed into PCA and then catabolized via the PCA cleavage pathway by the domesticated communities. PCA is one of the most common intermediates in the metabolic pathways of various aromatics [52]. Usually, PCA can be further catabolized via 4,5-cleavage (meta-cleavage), 3,4-cleavage (ortho-cleavage), and 2,3-cleavage pathways [52,53] by aerobic bacteria. We inferred that the domesticated communities mainly catabolized PCA via meta-cleavage and ortho-cleavage, as the corresponding critical catalyzing enzymes were identified in MAGs. Protocatechuate 4,5-dioxygenases composed of an alpha chain (ligA) and a beta chain (ligB) are responsible for catalyzing the meta-cleavage of PCA into 4-carboxy-2-hydroxy-*cis*,*cis*-muconate 6-semialdehyde [54]. The corresponding genes *ligA* and *ligB* were discovered in MAG1 (*Sphingomonas*), MAG3 (*Caballeronia*), and MAG4 (*Pigmentiphaga*), indicating their potential in meta-cleavage of PCA (Fig. 6). The ortho-cleavage of PCA is catalyzed by the protocatechuate 3,4-dioxygenase, which consists of two subunits (protocatechuate 3,4-dioxygenase alpha chain (*pcaG*) and protocatechuate 3,4-dioxygenase beta chain (*pcaH*)) [55]. Ten MAGs were identified to harbor both *pcaG* and *pcaH* with a potential capacity for PCA ortho-cleavage (Fig. 6). As shown in Fig. 6, the identified gene sequences of *pcaG* and *pcaH* formed three main clades in the phylogenetic tree. Genes *pcaG* and *pcaH* carried by MAG2 (*Cupriavidus*) and MAG3 (*Caballeronia*) were significantly enriched in the domesticated consortia (CAP-120c, PNB-100, and DCA-100) (*t* test,

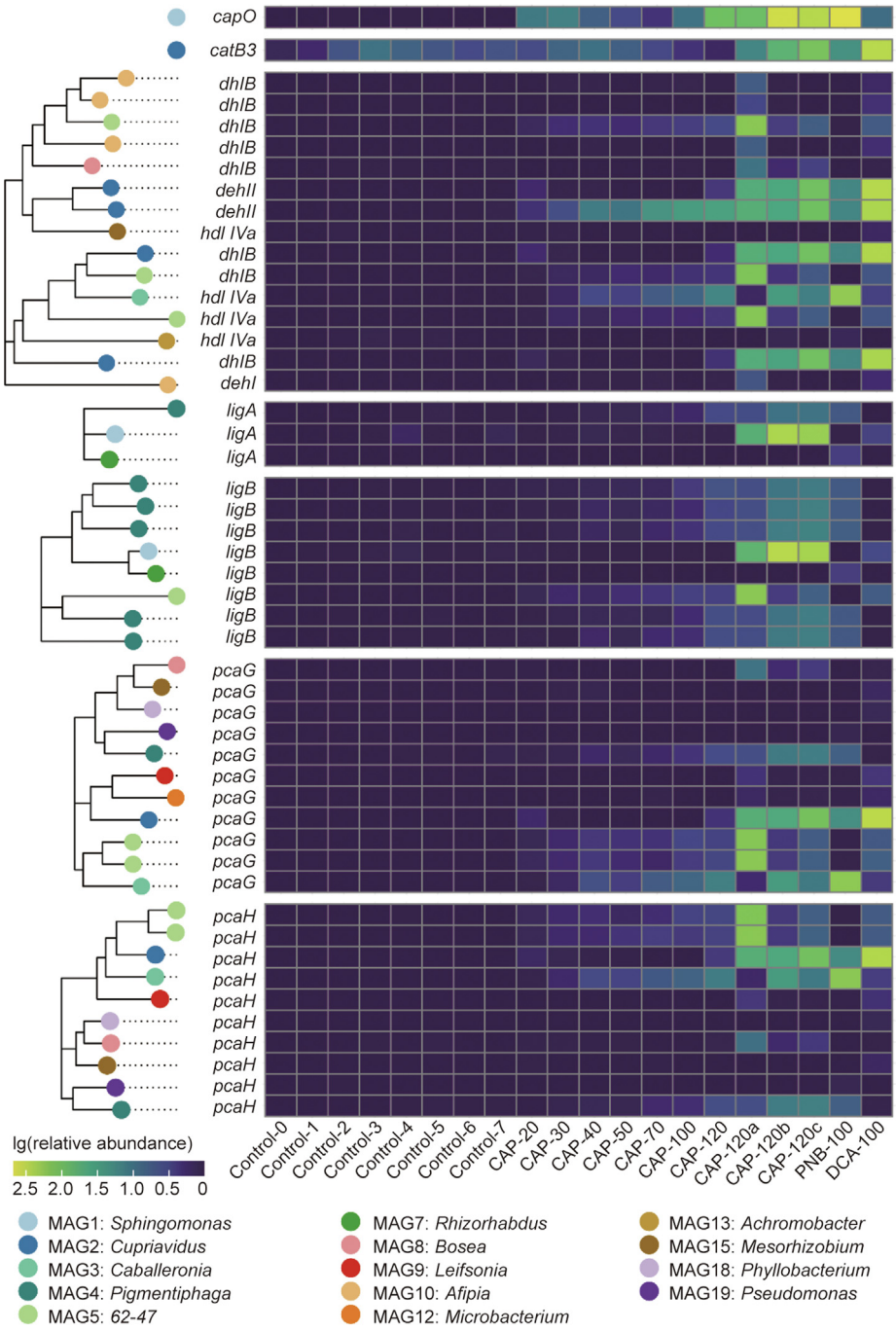

Fig. 6. The dynamic changes of the relative abundance (coverage, ×/Gb) of key genes involved in CAP, DCA, and PNB biotransformation in the communities during the domestication. The left cladogram depicts the phylogeny of genes in metagenomes. Colored bubbles in the phylogenetic tree indicate the corresponding gene carriers. *capO*: glucose-methanol-choline (GMC) oxidoreductase; *catB3*: chloramphenicol acetyltransferase; *dhlB*, *hdl IVa*, *dehII*, and *dehI*: haloacid dehalogenase; *ligA*: protocatechuate 4,5-dioxygenase alpha chain; *ligB*: protocatechuate 4,5-dioxygenase beta chain; *pcaG*: protocatechuate 3,4-dioxygenase alpha chain; *pcaH*: protocatechuate 3,4-dioxygenase beta chain. Values are presented as means of samples in groups.

$p < 0.05$). These results demonstrated the dynamic changes in the relative abundances of the critical genes involved in CAP, DCA, and PNB biotransformation during long-term domestication.

3.5. Impacts of environmental and nutrient factors on the CAP-degrading microbial community

Determining the factors influencing the performance of the CAP-degrading consortium is beneficial in guiding the design of the strategy for its application in the enhancement of CAP-contaminated environment bioremediation. Herein, the performance of CAP degradation by the domesticated CAP-degrading consortium CL-CAP under various environmental and nutrient conditions was investigate, and the results of CAP biodegradation and biomass of the consortium were shown in Figs. S4 and S5 in Appendix A. Moreover, the effects of the tested environmental and nutrient conditions on the populations of consortium CL-CAP were determined by 16S rRNA amplicon sequencing. As shown in Fig. S4(a), consortium CL-CAP degraded CAP faster as the initial inoculum size increased from 5% to 25%. It could completely

degrade 240 mg·L^{-1} CAP in 28 h at an initial inoculum size of 25%, which was more efficient than the known CAP degraders [12,16,56]. Consortium CL-CAP could completely degrade 240 mg·L^{-1} CAP at temperatures ranging from 20 to 30 °C, and it was fastest at 30 °C (Fig. S4(b)). The CAP-degrading efficiency of consortium CL-CAP was highest at a pH value of approximately 6.0, and the CAP degradation rate and cell growth were observably inhibited at pH values of 8.5 and 3.5 (t test, $p < 0.01$) (Figs. S4(c) and S5(c)). CAP at initial concentrations ranging from 50 to 400 mg·L^{-1} could be degraded entirely by the consortium, while CAP at initial concentrations higher than 500 m·L^{-1} was hard to degrade (Fig. S4(d)). CAP exerts antimicrobial effects by binding to the ribosomal 50S subunit, thereby impeding protein synthesis in bacteria [57]. When the CAP concentration is too high for community populations to detoxify in time, the growth of the community populations will be inhibited (Fig. S5(d)), and thereby, their substrate utilization rate will slow down.

Consortium CL-CAP was able to utilize CAP as the sole carbon and nitrogen source (Figs. S4(e) and (f)). The presence of additional carbon sources did not markedly accelerate the biodegradation of CAP by the consortium. CAP biodegradation was even hampered by sodium acetate, sodium citrate, and sodium benzoate (Fig. S4(e)). Remarkably, sodium acetate and sodium benzoate at concentrations higher than 12 mmol·L^{-1} significantly inhibited CAP biodegradation (t test, $p < 0.01$; Fig. S4(e)). Our previous study found that the growth of *Sphingomonas* sp. CL5.1, the critical CAP degrader in consortium CL-CAP, was significantly inhibited by 6 mmol·L^{-1} sodium acetate [13], which probably was a crucial obstructive factor for CAP biodegradation by the consortium. In addition, the biomass of community populations did not increase in the presence of 12 and 60 mmol·L^{-1} sodium benzoate (t test, $p < 0.01$; Fig. S5(e)). Sodium benzoate exerts broad-spectrum antimicrobial activity by interfering with the permeability of microbial cell membranes and inhibiting the activity of the respiratory enzyme system [58]. Thus, it is widely used in many foods and soft drinks as a preservative and antimicrobial agent [59]. Herein, the growth of the CAP-degrading consortium was intensely inhibited by sodium benzoate, which might serve as an approach for the control and disinfection of this consortium once it has completed its job for CAP removal. The inhibitory effect of nitrite nitrogen on CAP biodegradation and growth of the consortium was also observed (Figs. S4(f) and S5(f)). Several studies have reported that nitrite nitrogen has an inhibitory effect on bacterial growth and contaminant removal in biological wastewater treatment [60,61]. Nitrite nitrogen was proven to interfere with the cellular respiration of aerobic microbes by deactivating cytochrome oxidases or iron-containing enzymes [62].

The RDA suggested that the community was strongly affected by pH, initial CAP concentrations, and additional carbon sources (Adonis test, $p < 0.05$) (Figs. 7(a) and (b)). *Pigmentiphaga* and *Labrys* exhibited a positive relationship with pH (Fig. 7(a)). The relative abundance of *Labrys* was less than 0.5% at pH values of 4.5 and 6.0, while it was higher than 1.7% at pH values of 7.5 and 8.5. Moreover, *Labrys* even became a dominant member with an average relative abundance of 27.2% in the consortium at pH 8.5 (Fig. S6 in Appendix A). *Cupriavidus* showed a positive relationship with the initial CAP concentrations (Fig. 7(a) and Fig. S6). The community populations were intensely affected by additional carbon sources, including sodium acetate, sodium citrate, sodium pyruvate, and sodium benzoate, because of their dissimilar substrate preferences (Fig. 7(b) and Fig. S6). The demonstration of the impacts of environmental and nutrient factors on the CAP-degrading microbial community could guide the improvement of the biotreatment of CAP-polluted wastewater for better outcomes.

4. Conclusions

Biological treatment is a conventional and economical approach for antibiotic elimination in the practice of environmental bioremediation, such as wastewater treatment. The outcome is determined by the performance of functional microbes in the system. The performance of a biological treatment system can be enhanced via domestication with the corresponding antibiotic. Herein, three consortia with powerful CAP-, PNB- and DCA-degrading capacity

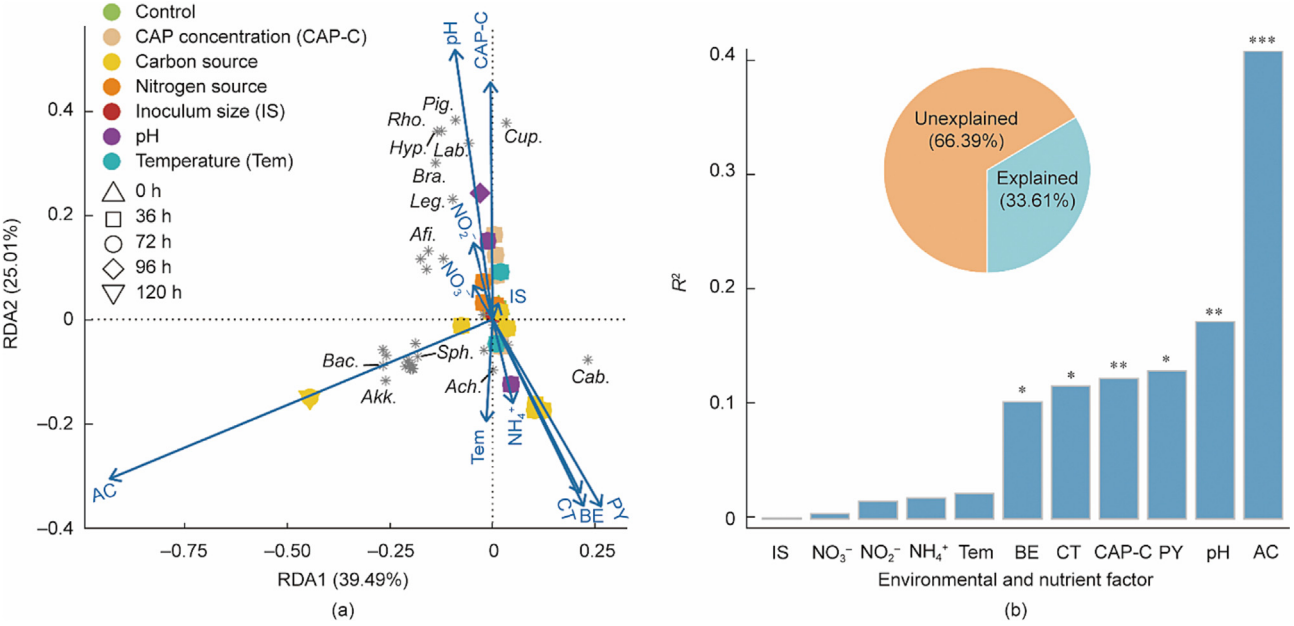

Fig. 7. The impacts of environmental and nutrient factors on the CAP-degrading microbial community. (a) Impacts of environmental and nutrient factors on the microbial community structures at genus level revealed by the RDA. (b) Adonis analysis determining the contribution of each environmental and nutrient factor on the microbial community structure. The pie shows the percentages of explained and unexplained variations. The tested carbon sources included sodium acetate (AC), sodium pyruvate (PY), sodium citrate (CT), and sodium benzoate (BE). The tested nitrogen sources included ammonium chloride (NH_4^+), sodium nitrate (NO_3^-), and sodium nitrite (NO_2^-). *Sph.*: *Sphingomonas*; *Cup.*: *Cupriavidus*; *Cab.*: *Caballeronia*; *Pig.*: *Pigmentiphaga*; *Lab.*: *Labrys*; *Bra.*: *Bradyrhizobium*; *Ach.*: *Achromobacter*; *Hyp.*: *Hyphomicrobium*; *Rho.*: *Rhodopseudomonas*; *Lei.*: *Leifsonia*; *Afi.*: *Afipia*; *Leg.*: *Legionella*; *Akk.*: *Akkermansia*; *Bac.*: *Bacteroides*; $^*p < 0.05$, $^{**}p < 0.01$, and $^{***}p < 0.001$.

were successfully domesticated from activated sludge. The successional pattern of microbial communities and critical genes of consortia through the 2.5-year domestication was characterized. Finally, *Sphingomonas* (57.8%), *Caballeronia* (60.2%), and *Cupriavidus* (74.5%) became dominators in the communities subsisting on CAP, PNB, and DCA in the MSM, respectively. Overall, the microbial diversity and evenness of consortia decreased through domestication. Crucial genes involved in CAP, PNB, and DCA metabolism were significantly enriched in consortia through long-term domestication. Environmental and nutrient factors such as pH and carbon source had observable impacts on the degradation efficiency, which should be considered for its further application in environmental bioremediation. *Sphingomonas*, *Caballeronia*, and *Cupriavidus* were the key degraders for CAP, PNB, and DCA in these consortia, respectively, due to their advantage of substrate utilization in communities. The domesticated consortia and isolated strains showed excellent performance on CAP, PNB, and DCA mineralization, which are important microbial resources for bioremediation. It should be noted that the stable colonizing capacity of the domesticated consortia and pure cultures in the practice of bioremediation should be further studied.

Acknowledgments

This study was funded by National Key Research and Development Program of China (2022YFE0103200), National Natural Science Foundation of China (22176107 and 22206107), Guangdong Basic and Applied Basic Research Foundation (2019B151502034 and 2021A1515110772), and China Postdoctoral Science Foundation (2021M691772).

Compliance with ethics guidelines

Jiayu Zhang, Kaiyan Zhou, Fangliang Guo, Huaxin Lei, Renxin Zhao, Lin Lin, Xiaoyan Li, and Bing Li declare that they have no conflict of interest or financial conflicts to disclose.

Appendix A. Supplementary data

Supplementary data to this article can be found online at https://doi.org/10.1016/j.eng.2023.07.009.

References

[1] Zhong M, Wang T, Zhao W, Huang J, Wang B, Blaney L, et al. Emerging organic contaminants in Chinese surface water: identification of priority pollutants. Engineering 2022;11:111–25.
[2] Chu W, Krasner SW, Gao N, Templeton MR, Yin D. Contribution of the antibiotic chloramphenicol and its analogues as precursors of dichloroacetamide and other disinfection byproducts in drinking water. Environ Sci Technol 2016;50(1):388–96.
[3] Li X, He F, Wang Z, Xing B. Roadmap of environmental health research on emerging contaminants: inspiration from the studies on engineered nanomaterials. Eco-Environ Health 2022;1(3):181–97.
[4] Zhang J, Xu J, Lei H, Liang H, Li X, Li B. The development of variation-based rifampicin resistance in *Staphylococcus aureus* deciphered through genomic and transcriptomic study. J Hazard Mater 2023;442:130112.
[5] Zhou Y, Farzana R, Sihalath S, Rattanavong S, Vongsouvath M, Mayxay M, et al. A one-health sampling strategy to explore the dissemination and relationship between colistin resistance in human, animal, and environmental sectors in Laos. Engineering 2022;15:45–56.
[6] Han Z, Feng H, Luan X, Shen Y, Ren L, Deng L, et al. Three-year consecutive field application of erythromycin fermentation residue following hydrothermal treatment: cumulative effect on soil antibiotic resistance genes. Engineering 2022;15:78–88.
[7] Tran NH, Chen H, Reinhard M, Mao F, Gin KY. Occurrence and removal of multiple classes of antibiotics and antimicrobial agents in biological wastewater treatment processes. Water Res 2016;104:461–72.
[8] Nguyen PY, Carvalho G, Reis MAM, Oehmen A. A review of the biotransformations of priority pharmaceuticals in biological wastewater treatment processes. Water Res 2021;188:116446.
[9] Wang G, Wang D, Xu Y, Li Z, Huang L. Study on optimization and performance of biological enhanced activated sludge process for pharmaceutical wastewater treatment. Sci Total Environ 2020;739:140166.
[10] Mosca Angelucci D, Clagnan E, Brusetti L, Tomei MC. Anaerobic phenol biodegradation: kinetic study and microbial community shifts under high-concentration dynamic loading. Appl Microbiol Biotechnol 2020;104(15):6825–38.
[11] Ma X, Qi M, Li Z, Zhao Y, Yan P, Liang B, et al. Characterization of an efficient chloramphenicol-mineralizing bacterial consortium. Chemosphere 2019;222:149–55.
[12] Ma X, Liang B, Qi M, Yun H, Shi K, Li Z, et al. Novel pathway for chloramphenicol catabolism in the activated sludge bacterial isolate *Sphingobium* sp. CAP-1. Environ Sci Technol 2020;54(12):7591–600.
[13] Zhang J, Gan W, Zhao R, Yu K, Lei H, Li R, et al. Chloramphenicol biodegradation by enriched bacterial consortia and isolated strain *Sphingomonas* sp. CL5.1: the reconstruction of a novel biodegradation pathway. Water Res 2020;187:116397.
[14] Sayed M, Khan A, Rauf S, Shah NS, Rehman F, Al-Kahtani A, et al. Bismuth-doped nano zerovalent iron: a novel catalyst for chloramphenicol degradation and hydrogen production. ACS Omega 2020;5(47):30610–24.
[15] Guo H, Jiang N, Wang H, Lu N, Shang K, Li J, et al. Degradation of antibiotic chloramphenicol in water by pulsed discharge plasma combined with TiO_2/WO_3 composites: mechanism and degradation pathway. J Hazard Mater 2019;371:666–76.
[16] Xin Z, Fengwei T, Gang W, Xiaoming L, Qiuxiang Z, Hao Z, et al. Isolation, identification and characterization of human intestinal bacteria with the ability to utilize chloramphenicol as the sole source of carbon and energy. FEMS Microbiol Ecol 2012;82(3):703–12.
[17] Grummt T, Wunderlich HG, Chakraborty A, Kundi M, Majer B, Ferk F, et al. Genotoxicity of nitrosulfonic acids, nitrobenzoic acids, and nitrobenzylalcohols, pollutants commonly found in ground water near ammunition facilities. Environ Mol Mutagen 2006;47(2):95–106.
[18] Liu Y, Li H, Wang R, Hu Q, Zhang Y, Wang Z, et al. Underlying mechanisms of promoted formation of haloacetic acids disinfection byproducts after indometacin degradation by non-thermal discharge plasma. Water Res 2022;220:118701.
[19] Zhao H, Yang L, Li Y, Xue W, Li K, Xie Y, et al. Environmental occurrence and risk assessment of haloacetic acids in swimming pool water and drinking water. RSC Adv 2020;10(47):28267–76.
[20] Zhao R, Yu K, Zhang J, Zhang G, Huang J, Ma L, et al. Deciphering the mobility and bacterial hosts of antibiotic resistance genes under antibiotic selection pressure by metagenomic assembly and binning approaches. Water Res 2020;186:116318.
[21] Zhang J, Li X, Klümper U, Lei H, Berendonk TU, Guo F, et al. Deciphering chloramphenicol biotransformation mechanisms and microbial interactions via integrated multi-omics and cultivation-dependent approaches. Microbiome 2022;10(1):180.
[22] Zhao R, Feng J, Huang J, Li X, Li B. Reponses of microbial community and antibiotic resistance genes to the selection pressures of ampicillin, cephalexin and chloramphenicol in activated sludge reactors. Sci Total Environ 2021;755(Pt 2):142632.
[23] Chen S, Zhou Y, Chen Y, Gu J. Fastp: an ultra-fast all-in-one FASTQ preprocessor. Bioinformatics 2018;34(17):i884–90.
[24] Wood DE, Lu J, Langmead B. Improved metagenomic analysis with Kraken 2. Genome Biol 2019;20(1):257.
[25] Lu J, Breitwieser FP, Thielen P, Salzberg SL. Bracken: estimating species abundance in metagenomics data. PeerJ Comput Sci 2017;3:e104.
[26] Nurk S, Meleshko D, Korobeynikov A, Pevzner PA. metaSPAdes: a new versatile metagenomic assembler. Genome Res 2017;27(5):824–34.
[27] Kolmogorov M, Bickhart DM, Behsaz B, Gurevich A, Rayko M, Shin SB, et al. metaFlye: scalable long-read metagenome assembly using repeat graphs. Nat Methods 2020;17(11):1103–10.
[28] Walker BJ, Abeel T, Shea T, Priest M, Abouelliel A, Sakthikumar S, et al. Pilon: an integrated tool for comprehensive microbial variant detection and genome assembly improvement. PLoS One 2014;9(11):e112963.
[29] Yu K, Qiu Z, Mu R, Qiao X, Zhang L, Lian CA, et al. Recovery of high-qualitied Genomes from a deep-inland Salt Lake Using BASALT. 2021. bioRxiv 2021.03.05.434042.
[30] Olm MR, Brown CT, Brooks B, Banfield JF. dRep: a tool for fast and accurate genomic comparisons that enables improved genome recovery from metagenomes through de-replication. ISME J 2017;11(12):2864–8.
[31] Parks DH, Imelfort M, Skennerton CT, Hugenholtz P, Tyson GW. CheckM: assessing the quality of microbial genomes recovered from isolates, single cells, and metagenomes. Genome Res 2015;25(7):1043–55.
[32] Chaumeil PA, Mussig AJ, Hugenholtz P, Parks DH. GTDB-Tk: a toolkit to classify genomes with the Genome Taxonomy Database. Bioinformatics 2019;36(6):1925–7.
[33] Hyatt D, Chen GL, Locascio PF, Land ML, Larimer FW, Hauser LJ. Prodigal: prokaryotic gene recognition and translation initiation site identification. BMC Bioinformatics 2010;11(1):119.
[34] Seemann T. Prokka: rapid prokaryotic genome annotation. Bioinformatics 2014;30(14):2068–9.

[35] Aramaki T, Blanc-Mathieu R, Endo H, Ohkubo K, Kanehisa M, Goto S, et al. KofamKOALA: KEGG Ortholog assignment based on profile HMM and adaptive score threshold. Bioinformatics 2020;36(7):2251–2.
[36] Joseph TA, Chlenski P, Litman A, Korem T, Pe'er I. Accurate and robust inference of microbial growth dynamics from metagenomic sequencing reveals personalized growth rates. Genome Res 2022;32(3):558–68.
[37] Ritchie ME, Phipson B, Wu D, Hu Y, Law CW, Shi W, et al. limma powers differential expression analyses for RNA-sequencing and microarray studies. Nucleic Acids Res 2015;43(7):e47.
[38] Bolyen E, Rideout JR, Dillon MR, Bokulich NA, Abnet CC, Al-Ghalith GA, et al. Reproducible, interactive, scalable and extensible microbiome data science using QIIME 2. Nat Biotechnol 2019;37(8):852–7.
[39] Wang Q, Garrity GM, Tiedje JM, Cole JR. Naive Bayesian classifier for rapid assignment of rRNA sequences into the new bacterial taxonomy. Appl Environ Microbiol 2007;73(16):5261–7.
[40] Nie M, Yan C, Xiong X, Wen X, Yang X, Lv Z, et al. Degradation of chloramphenicol using a combination system of simulated solar light, Fe_2^+ and persulfate. Chem Eng J 2018;348:455–63.
[41] Chen J, Xia Y, Dai Q. Electrochemical degradation of chloramphenicol with a novel Al doped PbO_2 electrode: performance, kinetics and degradation mechanism. Electrochim Acta 2015;165:277–87.
[42] Chong S, Song YL, Zhao H, Zhang GM, Li J. Ultrasound/Zn^0 for aqueous 4-nitrobenzoic acid degradation. Desalination Water Treat 2016;57(52):24990–8.
[43] Mazhar MA, Khan NA, Ahmed S, Khan AH, Hussain A, Rahisuddin, et al. Chlorination disinfection by-products in municipal drinking water—a review. J Clean Prod 2020;273:123159.
[44] Zhang J, Zhang H, Liu X, Cui F, Zhao Z. Efficient reductive and oxidative decomposition of haloacetic acids by the vacuum–ultraviolet/sulfite system. Water Res 2022;210:117974.
[45] Park KY, Choi SY, Ahn SK, Kweon JH. Disinfection by-product formation potential of algogenic organic matter from *Microcystis aeruginosa*: effects of growth phases and powdered activated carbon adsorption. J Hazard Mater 2021;408:124864.
[46] Luan X, Zhang H, Tian Z, Yang M, Wen X, Zhang Y. Microbial community functional structure in an aerobic biofilm reactor: impact of streptomycin and recovery. Chemosphere 2020;255:127032.
[47] Sorg RA, Lin L, van Doorn GS, Sorg M, Olson J, Nizet V, et al. Collective resistance in microbial communities by intracellular antibiotic deactivation. PLoS Biol 2016;14(12):e2000631.
[48] Zhang J, Li X, Lei H, Zhao R, Gan W, Zhou K, et al. New insights into thiamphenicol biodegradation mechanism by *Sphingomonas* sp. CL5.1 deciphered through metabolic and proteomic analysis. J Hazard Mater 2022;426:128101.
[49] Zhang J, Yang C, Hu J, Zhang Y, Lai Y, Gong H, et al. Deciphering a novel chloramphenicols resistance mechanism: oxidative inactivation of the propanediol pharmacophore. Water Res 2022;225:119127.
[50] Wang Y, Xiang Q, Zhou Q, Xu J, Pei D. Mini review: advances in 2-haloacid dehalogenases. Front Microbiol 2021;12:758886.
[51] Meusel M, Rehm HJ. Biodegradation of dichloroacetic acid by freely suspended and adsorptive immobilized *Xanthobacter autotrophicus* GJ10 in soil. Appl Microbiol Biotechnol 1993;40(1):165–71.
[52] Cao B, Nagarajan K, Loh KC. Biodegradation of aromatic compounds: current status and opportunities for biomolecular approaches. Appl Microbiol Biotechnol 2009;85(2):207–28.
[53] Kasai D, Fujinami T, Abe T, Mase K, Katayama Y, Fukuda M, et al. Uncovering the protocatechuate 2,3-cleavage pathway genes. J Bacteriol 2009;191(21):6758–68.
[54] Barry KP, Taylor EA. Characterizing the promiscuity of LigAB, a lignin catabolite degrading extradiol dioxygenase from *Sphingomonas paucimobilis* SYK-6. Biochemistry 2013;52(38):6724–36.
[55] Valley MP, Brown CK, Burk DL, Vetting MW, Ohlendorf DH, Lipscomb JD. Roles of the equatorial tyrosyl iron ligand of protocatechuate 3,4-dioxygenase in catalysis. Biochemistry 2005;44(33):11024–39.
[56] Xu H, Xiao L, Zheng S, Zhang Y, Li J, Liu F. Reductive degradation of chloramphenicol by *Geobacter metallireducens*. Sci China Technol Sci 2019;62(10):1688–94.
[57] Crofts TS, Sontha P, King AO, Wang B, Biddy BA, Zanolli N, et al. Discovery and characterization of a nitroreductase capable of conferring bacterial resistance to chloramphenicol. Cell Chem Biol 2019;26(4):559–70.
[58] Chen H, Zhong Q. Antibacterial activity of acidified sodium benzoate against *Escherichia coli* O157:H7, *Salmonella enterica*, and *Listeria monocytogenes* in tryptic soy broth and on cherry tomatoes. Int J Food Microbiol 2018;274:38–44.
[59] Khoshnoud MJ, Siavashpour A, Bakhshizadeh M, Rashedinia M. Effects of sodium benzoate, a commonly used food preservative, on learning, memory, and oxidative stress in brain of mice. J Biochem Mol Toxicol 2018;32(2):e22022.
[60] Liu B, Terashima M, Quan NT, Ha NT, Van Chieu L, Goel R, et al. High nitrite concentration accelerates nitrite oxidising organism's death. Water Sci Technol 2018;77(11–12):2812–22.
[61] Hrenović J, Orhan Y, Büyükgüngör H, Horvatiček M. Influence of ammonium, nitrate and nitrite on the performance of the pure culture of *Acinetobacter junii*. Biologia 2007;62(5):517–22.
[62] Rowe JJ, Yarbrough JM, Rake JB, Eagon RG. Nitrite inhibition of aerobic bacteria. Curr Microbiol 1979;2(1):51–4.